## Abstract

The bark represents the outer protective layer of trees and contains high concentrations of antimicrobial extractives. It also represents a side stream in forestry produced in millions of tons annually. In addition to cellulose, hemicelluloses, and lignin, spruce bark contains higher amounts of pectin and starch compared to spruce wood. Fungi are efficient lignocellulose degraders but their role in bark degradation is currently unclear. Cultivation of five fungi, *Dichomitus squalens*, *Rhodonia placenta*, *Penicillium crustosum, Trichoderma* sp. B1, and *Trichoderma reesei* on spruce bark over six months combined with chemical analyses of the bark revealed different degradation strategies. Toxic resin acids were degraded by Basidiomycetes but unmodified and tolerated by Ascomycetes. Substantial differences were also observed for glucuronoarabinoxylan and pectin degradation. The white-rot species *D. squalens* was further studied using proteomic analysis of its secreted proteins. Insight into fungal bark degradation strategies can inspire improved utilization of this abundant renewable resource.

Keywords: spruce bark, fungi, extractives, CAZymes, proteomics

## 1. Introduction

Bark is the outmost tissue of the tree, protecting it against abiotic stress, animal attack, and microbial degradation. The bark of trees accounts for around 10-15% of the volume at harvest, and approximately 400 million $m^3$ of bark are produced annually in the Nordic countries (Kwan et al., 2022), which mills and factories burn for energy. Similar to wood, the bark consists of lignin, hemicelluloses, and cellulose, but also additional compounds related to its protective role. The bark is enriched in molecules designated as extractive compounds (extractives), which, among other possible functions, may have anti-microbial properties (Kwan et al., 2022). The extractives vary greatly in amount and identity among tree species, and can also vary with growth stage and seasons (Ek et al., 2009). A softwood species of high industrial value in the northern hemisphere is spruce, and its bark has a low dry matter content compared to wood (Kemppainen et al., 2014), making direct combustion inefficient. It is however enriched in a diverse range of potentially valorizable extractives including triglycerides, steryl esters, sterols, resin acids, and fatty acids (Krogell et al., 2012), the most abundant of which are resin acids (~12 mg/g bark) that can be highly toxic due to interactions with biological membranes (Ek et al., 2009). The second-most abundant type of extractives is sterols, with β-sitosterol as the main compound.

Polysaccharides constitute ~40% (w/w) of spruce bark, but in addition to the expected wood polysaccharides, cellulose and hemicelluloses, the bark also contains notable amounts of starch and pectin (Krogell et al., 2012; Le Normand et al., 2012; Le Normand et al., 2021). Starch and cellulose are both homopolymers of D-glucose (Glc), but while cellulose features a linear β-(1→4)-linked backbone, starch is comprised of α-(1→4)-linked amylose and amylopectin with additional α-(1→6)-linked branch points. Of the bark dry weight, cellulose accounts for ~20-30%, and starch from 0.5 to several percent (Fengel & Wegener, 1984; Krogell et al., 2012). The primary hemicellulose in softwoods is galactoglucomannan (GGM), accounting for ~10% of the bark dry weight (Fengel & Wegener, 1984). GGM has a backbone of β-(1→4)-linked D-mannose (Man) and Glc units, which can be decorated with single α-(1→6)-linked D-galactose (Gal)

residues (Ek et al., 2009). The second most abundant hemicellulose in bark is glucuronoarabinoxylan (GAX), accounting for ~6% of the bark dry weight (Fengel & Wegener, 1984), which is comprised of a backbone of β-(1→4)-linked D-xylose (Xyl) residues which are commonly *O*-acylated and further substituted by α-(1→2)- and/or α-(1→3)-linked L-arabinose (Ara) and α-(1→2)-linked 4-*O*-methyl-glucuronic acid (4-*O*-MeGlcA) (Ek et al., 2009). Pectins are a heterogeneous group of complex charged polysaccharides – homogalacturonan (HG), xylogalacturonan (XG), and rhamnogalacturonans (RG-I and RG-II) – estimated to comprise 3-7% of the bark dry weight (Fengel & Wegener, 1984; Yadav et al., 2023). Of these, HG is the simplest, with an α-(1→4)-linked D-galacturonic acid (GalA) backbone that may be acetylated or methylated (Yadav et al., 2023). XG is a little more complex, featuring β-(1→3)-Xyl substitutions on the α-(1→4)-GalA backbone. In contrast, RG-II is regarded as the most structurally complex plant polysaccharide and is composed of at least ten different monosaccharides and a wide range of linkages. Pectins of the RG-I type have a backbone of alternating α-(1→4)-GalA and (1→2)-rhamnose (Rha) residues that can be decorated with extended galactan and arabinan sidechains.

Degradation of lignocellulosic material is a vital process within the carbon cycle and is mainly performed by fungi and bacteria capable of producing the required enzymatic arsenals. Among fungi, Basidiomycetes and Ascomycetes are recognized as major lignocellulose degraders. Within Basidiomycota, many species with broad lignocellulolytic potential are found and typically classified as either brown- or white-rot species depending on their effect on the wood. Brown-rot fungi rapidly depolymerize wood carbohydrates without significant removal of the brown-colored lignin, in contrast to the decay caused by white-rot fungi like *Dichomitus squalens*, which simultaneously degrade all wood components, including the recalcitrant, aromatic, and heterogeneous lignin polymer (Daly et al., 2018). Well known cellulase producers are found also within Ascomycete genera such as *Trichoderma*, *Aspergillus*, and *Penicillium*, and these can exhibit another type of lignocellulose degradation called soft-rot. As the name implies, soft-rot leads to an overall softened structure upon degradation, and is further categorized into type 1 and

2, where the former involves formation of longitudinal cavities within secondary cell walls, and the latter leads to full secondary cell wall degradation (Kubicek, 2012).

In comparison to the microbial degradation of wood and other lignocellulosic materials, there is limited knowledge regarding the biological degradation of bark and its extractives. One early proteomic study examined the secretome of the filamentous fungus *Aspergillus nidulans* growing on cork oak bark using 2D gel electrophoresis, though only for a single timepoint (Martins et al., 2014). Two white-rot fungi, *Phanerochaete velutina* and *Stropharia rugosoannulata*, were found to degrade hemicelluloses, cellulose, and certain extractives when grown on Scots pine bark, although the specific compounds degraded by these fungi were not examined (Valentín et al., 2010). The brown-rot fungus *Rhodonia placenta* (formerly *Postia placenta*) has additionally been shown to degrade resin acids (Belt et al., 2017). Somewhat more detailed knowledge exists regarding extractive degradation by the white-rot fungus *Phlebiopsis gigantea*, which can metabolize non-toxic triglycerides from bark (Hori et al., 2014). There are no studies comparing the growth of multiple filamentous fungi, from both Ascomycetes and Basidiomycetes, on spruce bark over time, with simultaneous monitoring of the resulting chemical changes to the bark.

In this study, we have followed the degradation of spruce bark by five fungi representing different lignocellulose degradation strategies: *Dichomitus squalens* (white-rot), *Rhodonia placenta* (brown-rot), *Trichoderma reesei* (soft-rot), *Penicillium crustosum* (mold), and a new *Trichoderma* strain isolated from a spruce tree stump. Their growth on spruce bark was monitored over six months and coupled to chemical compositional analyses to evaluate the impact of growth on the bark extractives, lignin, and polysaccharides. Bark degradation by *D. squalens* was studied in more detail, which revealed remarkable proficiency in degrading hemicelluloses and pectin, the primary non-cellulose polysaccharides found in spruce bark. Proteomic analysis of the *D. squalens* secretome during bark deconstruction revealed putative novel extractive-degrading enzymes and carbohydrate-active enzymes (CAZymes).

## 2. Material and methods

### *2.1 Maintenance and identification of fungi*

Dikaryotic *Dichomitus squalens* strain FBCC312 (CBS 432.34), *Rhodonia placenta* (CBS 447.48), *Trichoderma reesei* (NCIM 1186), *Penicillium crustosum* (FRR 1669) were maintained on Potato dextrose agar (PDA) plates (Sigma). The fungal strain B1 was isolated from a spruce tree stump just below the partly degraded bark (summer of 2019, Hälsingland county, Sweden), and cultivated on PDA plates until a uniform culture was obtained. For identification, genomic DNA was extracted using the NucleoSpin Soil kit (Macherey-Nagel). The ITS gene region was amplified using PCR with extracted DNA as a template and ITS primers ITS1 (5'-TC CGT AGG TGA ACC TGC GG-3') and ITS4 (5'-TCC TCC GCT TAT TGA TAT GC-3'), as well as the EF1-α gene using the primers EF1-728F (5'-CAT CGA GAA GTT CGA GAA GG-3') and EF1-986R (5'-TAC TTG AAG GAA CCC TTA CC-3') (Carbone & Kohn, 1999; Jaklitsch et al., 2005; Martin & Rygiewicz, 2005). The PCR mixture (50 µL) contained Maxima Hot Start PCR Master Mix (Thermo), 0.5 µM of each primer, and 1 µL of extracted genomic DNA. The PCR protocol was: 94 °C for 3 min, 30 cycles of 94 °C for 30 s, 55 °C for 30 s, and 72 °C for 1 min, followed by a final extension at 72 °C for 10 min. The sequenced PCR products (Macrogen) were compared with those deposited in the GenBank database using the NCBI BLAST program.

### *2.2 Fungal cultivation on bark*

For each fungus, static liquid pre-cultures in 250 ml Erlenmeyer flasks containing 50 mL potato dextrose broth (Sigma) were inoculated from PDA plates with three agar plugs (0.5 cm diameter) and incubated for 7 days at 20 °C. Mycelium from two of the static pre-cultures was fished out with an inoculating loop and transferred to a blender cup that was filled with 150 ml basal medium (4 g/L $KH_2PO_4$, 13.6 g/L $(NH_4)_2SO_4$, 0.8 g/L $CaCl_2 \cdot 2H_2O$, 0.6 g/L $MgSO_4 \cdot 7H_2O$, 10 mg/L $FeSO_4 \cdot 7H_2O$, 3.2 mg/L $MnSO_4 \cdot H_2O$, 2.8 mg/L $ZnSO_4 \cdot 7H_2O$, 4 mg/L $CoCl_2 \cdot 6H_2O$) and blended in a Waring blender for 10 s at 8000 rpm three times with a 30 s pause in between each blending (Daly et al., 2018). From the blended precultures, 1 ml was mixed with 35 mL of basal medium

in a 50-mL tube and added to 10 g of gamma-irradiated spruce bark (25 kGy, Mediscan GmbH & Co) (Ristinmaa et al., 2023) on plates, and then weighed. A total of five cultures were incubated at 20 °C for each time-point: three for compositional analysis experiments and two for mass loss measurements. Separate control bark samples were dried for three days at 60 °C, and then weighed. To account for mass loss after fungal degradation the weight of each sample was compared to the weight of the starting material.

### *2.3 Compositional analysis of spruce bark*

All compositional data in the graphs in this paper was assessed based on the percent change compared to the control (blank) sample measured at the same week (Equation 1), below.

$$\% \, \boldsymbol{Change} = \frac{\boldsymbol{X_1} - \boldsymbol{X^b_{mean}}}{\boldsymbol{X^b_{mean}}} \qquad \textbf{(1)}$$

$X_1 =$ measured values at week y

$X^b_{mean} =$ the mean of the three blank samples at week y

#### *2.3.1 Ash content*

The proportion of ash present in the bark was measured according to the National Renewable Energy Laboratory standard method as previously described (Ristinmaa et al., 2023).

#### *2.3.2 Extractive extraction, analysis, and quantification*

For evaluation of the effect of microbial growth on the spruce bark extractives, Soxhlet extraction was used, as previously described (Ristinmaa et al., 2023). Gas chromatography coupled to mass spectrometry (GC-MS; Agilent 7890A and Agilent 5975C) with a quadrupole was used to identify and quantify individual bark extractives. Concentrations were determined using an internal methyl heptadecanoic standard and pure external standards. All fatty acids were quantified against hexadecenoic acid, all resin acids against dehydroabietic acid, and β-sitosterol against pure standard. Response factor for isopimarane type resin acids were determined by performing silylation and GC analysis on two samples containing equal amounts of 0.1 mg/L isopimaric acid, hexadecenoic acid, and dehydroabietic acid. Bark extractive samples were dissolved in acetone

to 10 mg/mL. From this, 300 µL was mixed with 200 µL of internal standard (methyl heptadecanoic acid, 1 mg/mL) in acetone. Thereafter, the bark extracts and standards were derivatized with 100 µL *N*-Methyl-*N*-(trimethylsilyl)trifluoroacetamide (TMS), heated for 20 min at 70 °C, and then analyzed as trimethylsilyl derivatives. Helium was used as carrier gas with a flow rate of 1 mL/min. The MS source was operated at 230 °C and the quadrupole at 150 °C. Analytes were separated using a HP-5 column (Agilent) with an injector temperature set to 300 °C, the temperature program starting at 70 °C, and this was held for 2.25 min, then increased to 200 °C at 20 °C/min, and thereafter increased to 230 °C at 5 °C/min. The final ramp was at 35 °C/min to 300 °C which was then held for 10 min. The NIST MS Search Program (v. 2.2) was used for identification using the NIST/EPA/NIH Mass Spectral Library (NIST 11), in addition to external standards (see supplementary material).

### *2.3.3 Protein content*

The protein content of the acetone extracted bark was derived from measuring the nitrogen content using CHNS combustion analysis (Elementar vario MICRO cube), using helium as the carrier gas. After drying at 105 °C overnight, ~2 mg of the bark was weighed in tin weighing boats. The contents of carbon, hydrogen, nitrogen, and sulfur were determined. Calibration was done using sulphanilamide (Elemental Microanalysis), and combustion and reduction were conducted at 1,150 and 850 °C, respectively. The protein content was estimated by multiplying the measured nitrogen content with the nitrogen to protein conversion factor 6.25 (Jones, 1931).

### *2.3.4 Chemical characterization of carbohydrates and lignin*

To elucidate if the fungi were degrading carbohydrates or lignin in the spruce bark, the acetone-extracted bark was dried overnight at 105 °C, followed by hydrolysis using 72% (w/w) sulfuric acid, as previously described (Ristinmaa et al., 2023). The monosaccharide concentrations were determined using an internal fucose standard and pure external standards of Rha, Ara, Man, Gal, Glc, Xyl, using HPAEC-PAD. Peak analysis was performed using Chromeleon software 7.2.10 (Thermo Scientific). Total starch in the bark was analyzed using the total starch assay kit from

Megazyme (Ireland), using the standard protocol with minor modifications. The sample was dried for three days at 50 °C to prevent formation of retrograde starches. Sample amounts were decreased four-fold, with all ratios equal. Glucose concentrations were determined using HPAEC-PAD, as described above. To analyze non-crystalline oligo- and polysaccharides, about 10 mg per freeze-dried bark sample was weighed, subjected to methanolysis, and analyzed as silylated sugars by GC, as previously described, except that resorcinol was used as an internal standard (Krogell et al., 2013).

### *2.4 Proteomic sample preparation and analysis*

The monokaryotic *D. squalens* strain CBS 464.89 (Westerdijk Fungal Biodiversity Institute), which is a direct offspring of the dikaryon FBCC312, was maintained on plates containing 2% (wt/vol) malt extract and 1.5% (wt/vol) malt extract agar (MEA) (Sigma). Two-layer agar plates including a filter disc were prepared as previously described (Bengtsson et al., 2016), with the exception that a sterile QM-A Quartz filter, 47 mm diameter (Cytiva) was used to facilitate separation of cells from secreted proteins, as previously described (Bengtsson et al., 2016). Plates were prepared using basal medium (as described in above) and 1.5% (wt/vol) agar, and 10 g/L carbon source: spruce bark, acetone-extracted spruce bark (extractive free), glucose (Sigma), galactomannan (Sigma), or cellulose (Sigma, microcrystalline, powder, 20 μm), respectively. Secretomes from cells grown on plates were collected after 9 days. The sample preparation was done as previously described (Lorentzen et al., 2021), except that a disc of agarose, with a total volume of approximately 2 mL, was punched out from the underside of the agar disc using the back end of a 50-mL tube against the center of the membrane, before extraction and trypsination of peptides. The tryptic peptides were analyzed by liquid chromatography combined with mass spectrometry (LC-MS/MS; 5 μL per injection) as described below. Peptides were analyzed as previously described (Lorentzen et al., 2021), using a Dionex Ultimate 3000 nanoLC-MS/MS system connected to a Q-Exactive mass spectrometer (both from Thermo Scientific) equipped with a nano-electrospray ion source.

MS raw files were analyzed using MaxQuant version v2.4.2.0 and proteins were identified and quantified using the MaxLFQ algorithm. The data were searched against the UniProt proteome of *D. squalen*s (UP000292082; 15,221 sequences) supplemented with common MS and proteomics contaminants such as keratins and bovine serum albumin. In addition, reversed sequences of all protein entries were concatenated to the database for estimation of false discovery rates (FDR). The tolerance levels for matching to the database were 6 ppm for MS and 20 ppm for MS/MS. Two missed cleavages by trypsin were allowed. Protein N-terminal acetylation, oxidation of methionines, deamidation of asparagines and glutamines and formation of pyro-glutamic acid at N-terminal glutamines were allowed as variable modifications. The 'match between runs' feature of MaxQuant, which enables identification transfer between samples based on accurate mass and retention time, was applied with default settings. A protein was considered identified by the following procedure: all search results provided by MaxQuant were filtered to achieve a protein FDR of 1% and only proteins present in at least two of the three biological replicates per growth substrate were kept for further analysis. Perseus version 1.6.1.1 was used for data analysis and R v.2023.03.0 was used for visualization. Protein secretion was predicted using a combination of three prediction algorithms: SignalP version 6.0 (https://www.cbs.dtu.dk/services/SignalP/) and Phobious (https://phobius.sbc.su.se/) using default parameters for eukaryotic species, and WolfPSort (https://wolfpsort.hgc.jp/) using a fungal prediction pattern. A protein was considered secreted if predicted by at least two of the three algorithms. Protein names used throughout the manuscript were assigned by UniProt and further annotated with CAZy family numbers, including carbohydrate-binding modules, using dbCAN2 (Zhang et al., 2018) with CAZy hidden Markov models, as well as with Enzyme Commission (EC) numbers and gene ontology (GO) terms, when available, downloaded from UniProt.

## 3. Results and Discussion

To gain insight into fungal degradation of bark, fresh spruce bark was collected, partially dried, milled and subjected to sterilization using gamma-irradiation rather than autoclaving, which would cause chemical changes. Five fungi from both Basidiomycota and Ascomycota were inoculated onto replicate bark samples, which were then collected over a 24-week period, during which visible mycelial growth was observed for each species (Fig. 1). To cover different types of lignocellulose degradation, the chosen species were, from both Ascomycota and Basidiomycota. The Ascomycota were two *Trichoderma* species and one *Penicillium*. *T. reesei* was chosen as an industrially important cellulolytic filamentous fungus. Additionally, a new fungal strain was used in the study, which was sourced from a spruce tree stump (underneath the bark). It was identified as a *Trichoderma* species, by re-streaking until a monoculture was observed on plates followed by amplifying and sequencing the ITS region and the EF1-α gene, which showed the closest match to *Trichoderma* in NCBI (98.89% seq. id. and 99% query cover for EF1-α to *Trichoderma atroviride* and 100% for ITS to *Trichoderma paraviridescens*). This strain was designated as *Trichoderma* sp. B1, and its ITS and EF1-α sequences have been deposited in NCBI under accession numbers OQ875786 and OQ918064, respectively. The third Ascomycete, initially discovered as a rapidly growing green contaminant in some bark samples, was identified as *Penicillium crustosum* in a similar fashion, for which the type strain was then ordered and used. Two Basidiomycetes were additionally selected: the well-studied white-rot fungus *D. squalens*, and the brown-rot fungus *R. placenta*.

### *3.1 Fungal growth on spruce bark*

The growth of microorganisms was assessed over time by measuring the overall mass loss of the samples by comparison to the initial weights. Regardless of the fungus used, clear degradation of the bark was observed, though the extent of mass loss varied among the fungi. *D. squalens* caused the highest mass loss, with 30% at the end of the experiment and reaching an apparent stationary phase (i.e., minor additional weight loss) within 12 weeks. For *T. reesei*, the total mass loss

reached 20% and stationary phase was reached within 16 weeks, while *Trichoderma* sp. B1 reached 26% mass loss but only reached a stationary phase after 20 weeks (Fig. 1). Compared to the other fungi *R. placenta* and *P. crustosum* showed shorter lag phase, which indicates quick colonization of the bark. The total mass loss for *R. placenta* was comparable to *T. reesei* at ~20%, but the fast bark colonization of *P. crustosum* surprisingly resulted in the lowest overall mass loss (14%) of the fungi. It is important to note that the actual degradation of the bark is likely higher than the reported mass loss, as the mass loss does not account for conversion of bark into microbial biomass; these measurements only reflect the conversion of bark to volatile compounds such as $CO_2$. The distinct growth profiles of the five fungi (Fig. 1) suggest different substrate preferences, which was further evaluated through compositional analyses of the bark. The observed variations in growth may also reflect differences in tolerance of extractives for each species, as many of these compounds are known to inhibit fungal growth (Belt et al., 2017; Kirker et al., 2013).

### *3.2 Bark decomposition*

The fungal bark degradation was evaluated by compositional analysis at three time points (week 0, 12, and 24), representing early-, mid-, and late stages of degradation. In correlation with the observed mass loss in the samples, the proportional ash content in the bark increased significantly in all biotic samples compared with the uninoculated control, indicating significant loss of material in the form of $CO_2$ or other volatiles (Fig. 2; supplementary material). *D. squalens*, *T. reesei*, and *Trichoderma* sp. B1 exhibited the highest apparent increase in ash content, reaching up to 40% at week 24 (Fig. 2). All measured compounds were evaluated against the total amount of ash rather than the dry bark weight, to account for the mass loss resulting from the production of volatiles, as in previous long-term bark degradation studies by microbial consortia (Ristinmaa et al., 2023). Protein content can be used as an estimate of fungal growth and was indeed shown to increase in all samples (Fig. 2). *D. squalens* had the highest total protein content after six months, which again suggests better growth compared to the other fungi.

Lignin degradation was evaluated by measuring Klason and acid-soluble lignin (Fig. 2). Over time, the content of acid-soluble lignin decreased in samples treated with *D. squalens* and *Trichoderma* sp. B1, while it increased in samples treated with the other fungi. In contrast, Klason lignin degradation was minimal, even for well-known degraders of lignin such as *D. squalens* (Daly et al., 2018). Only minor evidence of degradation of Klason lignin was observed for the two Ascomycetes *P. crustosum* (after 12 weeks) and *T. reesei* (after 24 weeks). Due to the inherent difficulties in accurately quantifying lignin in a complex sample, further verification would be needed to confirm lignin degradation, for instance by using pyrolysis−GC−MS in combination with 2D-NMR (van Erven et al., 2017).

### *3.3 Degradation of extractives*

The bark extractives, which are known for their antimicrobial properties, were expected to undergo modification and/or degradation during fungal growth. Indeed, a significant decrease in the total extractive content was seen across all fungal cultures (Fig. 2). To gain further insight into changes in specific extractives, additional analysis was conducted using GC-MS to monitor the most abundant fatty acids, resin acids, and sterols, which were identified using standards if available (hexadecanoic acid, isopimaric acid, dehydroabietic acid, abietic acid, β-sitosterol) or putatively identified by using the NIST library (9,12-octadecadienoic acid, octadecanoic acid, pimaric acid, 7-oxodehydroabietic acid, and ergosterol). All compounds identified by NIST had a match factor above 800, except ergosterol which had a match factor of 716. For the ten components assessed, all fungi caused either an increase or a decrease of at least one of the compounds, compared to the control sample. Changes in the contents of four selected compound types, with representatives from abietane and pimarane type resin acids, fatty acids, and sterols, are shown in Fig. 2. All the identified fatty acids (hexadecenoic acid, linolenic acid, 9,12-octadecanoic acid, trans-9-octadecanoic acid) appeared to be readily available carbon sources for all fungi and were nearly entirely consumed at 12 weeks (see supplementary material).

296 The resin acid dehydroabietic acid, the most abundant extractive component (9.9 mg/g bark), was
297 efficiently converted by *D. squalens* and *R. placenta* resulting in an 80% reduction after 12 weeks
298 of growth. The same trend was found for abietic acid, isopimaric acid, and pimaric acid, while 7-
299 oxodehydroabietic acid was not identified in these samples. Previous studies have shown that *R.*
300 *placenta* degrades resin acids during growth on Scots pine wood (Belt et al., 2022). Interestingly,
301 much smaller, and in some cases minimal effects on the levels of all resin acids were observed
302 for the three Ascomycetes, *P. crustosum*, *Trichoderma* sp. B1, and *T. reesei*. This not only
303 indicates an inability to degrade or modify resin acids, but also tolerance to their inhibitory effects.

304 The data show that among the fungi, only *D. squalens* and *R. placenta* could degrade the
305 pimarane-type resin acid isopimaric acid, in addition to abietic acid. Resin acid degradation has
306 been more investigated for bacteria, for which ability to degrade both pimarane and abietane resin
307 acids is very rare (Martin et al., 1999). Pimarane type resin acids are considered more toxic and
308 resistant to degradation compared to abietane types (Martin et al., 1999), making the similar
309 degradation of both types by the Basidiomycetes used in this study an interesting observation that
310 could be studied further. However, we cannot currently determine whether the resin acids
311 underwent complete degradation/metabolism or were transformed into less harmful metabolites
312 that escaped detection. The mechanisms underlying the tolerance of the Ascomycetes towards
313 resin acids are currently unclear, though a previous study comparing the transcriptome of *P.*
314 *gigantea* grown on untreated and acetone-extracted milled loblolly pine wood showed
315 upregulation of ABC efflux transporters for the former, which may contribute to such tolerance
316 (Hori et al., 2014). To the best of our knowledge, this is the first report highlighting marked
317 differences in bark extractive responses across different fungal taxa.

318 As expected, ergosterol was identified in the fungal-treated bark samples but not in the control
319 which is expected as it is a fungal cell membrane sterol. The most abundant bark-derived sterol,
320 β-sitosterol, with an initial abundance of 2.6 mg/g bark, increased in cultures inoculated with *P.*
321 *crustosum, D. squalens*, and *Trichoderma* sp. B1 (Fig. 2). This suggests that these fungi possess

steryl esterases and can metabolize the released fatty acids but have limited ability to further degrade β-sitosterol itself. In contrast, *R. placenta* and, to a lesser extent, *T. reesei* were able to degrade β-sitosterol, indicating that they can metabolize both sterols and steryl esters. Steryl esters were unfortunately not possible to measure directly using our experimental setup.

### *3.4 Degradation of carbohydrates*

To gain a comprehensive understanding of overall polysaccharide degradation, all samples were subjected to sulfuric acid hydrolysis followed by monosaccharide quantification using HPAEC-PAD (Fig. 3). The degradation of glucuronoarabinoxylan (GAX) and pectin was assessed by measuring the change in Xyl and Rha, for which the initial contents were 28.17 mg/g bark and 6.4 mg/g bark, respectively (see supplementary material). Regarding the consumption of these polysaccharides, major differences were observed. *D. squalens* and *P. crustosum* rapidly consumed Rha, a major component of the pectin main chain, in contrast to the two *Trichoderma* species. After 12 weeks, the white-rot *D. squalens* exhibited significant removal of Xyl (64%) and Rha (66%), indicating efficient degradation of both GAX and pectin. In contrast, the other Basidiomycete *R. placenta* displayed a clear preference for pectin degradation, with a similar removal of Rha (47% and 62% at week 12 and 24, respectively) as *D. squalens*, but with much less removal of Xyl (15% and 32% after 12 and 24 weeks). *P. crustosum* exhibited an even greater preference for early-stage pectin degradation, removing 66% of Rha at week 12, compared to 23% for Xyl. In contrast to these three fungi, the two *Trichoderma* species showed limited degradation of pectin, Rha (~27% removal after 24 weeks) and a preference for GAX degradation (~60% Xyl removal after 24 weeks). *T. reesei* is not known as a potent pectin degrader (Gao et al., 2022), but evaluation of the growth of *Trichoderma* sp. B1 on pectin in agar plates demonstrated robust growth on polymethylgalacturonan (unpublished results). It is conceivable that spruce bark pectins are too complex for efficient depolymerization by this fungus, possibly due to a limited capacity for side chain removal which would hamper degradation of the main chain. In contrast to pectin degradation, xylan metabolism showed relatively consistent patterns

among all fungi, except for *R. placenta*, which displayed low xylan degradation compared to the others.

Ara and Gal occur in the main-chain decorations of both pectin and the hemicelluloses GAX and GGM. After complete sulfuric acid hydrolysis, it is not possible to conclusively determine from where these monosaccharides originate (i.e., pectin or hemicellulose). The initial relative abundances of Ara and Gal were 56.8 mg/g bark and 22.7 mg/g bark, respectively (see supplementary material). Ara degradation was observed for all five fungi, indicating the presence of functional arabinofuranosidases acting on GAX (Fig. 3). In contrast, the degradation of Gal varied among the fungi. *D. squalens* appeared to reach its maximal degradation already at week 12 (64% removal). Gal removal was less extensive for the other fungi, ranging from approximately 25% to 50% after 24 weeks.

The removal of Man (initial amount 20.65 mg/g), derived from galactoglucomannan, was seemingly limited for all fungi, with *D. squalens* displaying the highest removal (37% after 12 weeks). Importantly, consumption of bark-derived Man is likely underestimated to some extent because mannan is a major component also of fungal cell walls, and separation of fungal and bark biomass was not possible in our experimental setup.

While previous studies indicate that starch can constitute a significant fraction of spruce bark (Krogell et al., 2012), the reported values vary and can be as low as 0.5% (Kemppainen et al., 2014; Le Normand et al., 2012). Similarly, the bark used here had low starch content, initially 5.41 mg/g (see supplementary material), which means that starch is unlikely to serve as a significant energy source during fungal growth. Starch is regarded as an accessible carbon source, and as anticipated, *R. placenta*, *Trichoderma* sp. B1, and *P. crustosum* degraded about 90% of it by week 12 (Fig. 3). Intriguingly, *T. reesei* showed no starch degradation, and *D. squalens* appeared to only have initiated this process after twelve weeks. These results may however reflect accumulation of fungal glycogen, which would lead to underestimation of starch degradation, as

these polysaccharides cannot be distinguished using our analytical approach. The remaining glucose ($Glc_{corr}$), initially 243.7 mg/g (see supplementary material) when corrected for apparent starch content, is comprised of Glc from cellulose, hemicellulose (GGM or possibly xyloglucan, XyG), and could at later stages also be derived from fungal β-glucans. By week 12, *D. squalens* achieved the highest apparent removal of Glc from the bark (64%), with *Trichoderma* sp. B1 (56%), and *Trichoderma reesei* (55%) reaching similar levels. In contrast, *R. placenta* and *P. crustosum* only achieved 25% degradation at 24 weeks.

In a previous study of microbial consortia growing on bark, in which degradation appeared dominated by bacteria, carbohydrate turnover was minimal, despite the presence of Ascomycetes and Basidiomycetes (Ristinmaa et al., 2023). In contrast, when we here inoculated spruce bark with isolated fungi, we observed significant degradation of polysaccharides during growth. The observation that a single fungal species can thrive on the bark while a consortium takes considerably longer may be attributed to factors such as competition or direct bacterial inhibition of fungi. Additionally, in the present study, we utilized a basal medium containing trace metals designed for optimal fungal growth, whereas the previous study on microbial communities employed a minimal medium (M9) which could be more appropriate for bacterial growth.

As *D. squalens* was found to grow well on the bark, and was able to degrade all polysaccharides, methanolysis was employed to gain deeper insight into its hemicellulose and pectin degradation. Consistent with the previous findings, the change in monosaccharide levels between weeks 12 and 24 was minimal, indicating that degradation of hemicelluloses and pectin primarily occurs during the initial stages of cultivation (see supplementary material). Methanolysis enabled the measurement of additional monosaccharides, such as 4-*O*-MeGlcA and GalA (see supplementary material). Both 4-*O*-MeGlcA and Xyl, which are associated with GAX (initial levels: 2.9 mg/g and 29 mg/g, respectively) decreased to similar extents (34% and 44% removal, respectively) after 12 weeks. Regarding pectin, there was clear removal of GalA (67%) and Rha (60%) at week 12 (initial levels: 56 mg/g and 8.9 mg/g, respectively). The decline in Ara (70%; initial amount

66.7 mg/g) and Gal (55%; initial amount 27 mg/g) (see supplementary material) implies that breaking down Ara- and Gal-containing decorations on hemicellulose and pectin enhances subsequent polysaccharide hydrolysis, in agreement with previous studies on enzymatic accessibility to polysaccharides (Clarke et al., 2000). The measurements of D-glucuronic acid (GlcA; initial amount 2.3 mg/g) were highly variable making its estimated removal (27%) inconclusive. The methanolysis provides additional insight into cellulose degradation, which may be obtained by subtracting the total glucose concentration (sulfuric acid hydrolysis) from non-cellulosic glucose (methanolysis). The data indicate that cellulose degradation ceased after 12 weeks when 61% had been converted (timepoint zero = 159 mg/g).

### *3.5 Secretome composition during growth of D. squalens on spruce bark*

Based on the compositional analysis results, it was evident that *D. squalens* displayed rapid growth on spruce bark and effectively degraded both extractives and polysaccharides. To further investigate which proteins the fungus produced during the degradation process, proteomics analysis was conducted. *D. squalens* was cultivated using five different carbon sources: spruce bark (Bark), acetone extracted spruce bark (extractive free; ACB), cellulose, galactomannan (GM), and glucose. A previously established plate method that facilitates the separation of secreted proteins (the secretome) and fungal biomass was employed (Bengtsson et al., 2016).

For the prediction of secreted proteins in the complete proteome of *D. squalens*, an analysis combining Phobius, SignalP, and WolfPsort was conducted, and proteins were annotated as extracellular if identified as such by at least two of these predictors (Horton et al., 2007; Käll et al., 2004; Teufel et al., 2022), and this analysis showed the fraction of secreted proteins in the whole proteome being 7.5%. A total of 1,139 proteins were identified in the experimental secretome, of which 193 (17%) were annotated as extracellular (see supplementary material). The fraction of extracellular proteins varied between substrate, from 40% for cellulose to approximately 17% for ACB, Bark and GM. These numbers show that lysis had occurred during growth on all substrates, albeit to different extents. For filamentous fungi, the plate method used

here has shown varying degrees of enrichment of secreted proteins, depending on carbon source (Arntzen et al., 2020), and given the observed lysis in these samples, we limited further analysis to predicted extracellular proteins (see supplementary material).

### *3.6 Detected extracellular CAZymes produced by D. squalens*

The secretomes were analyzed using dbCAN2 v11 (Zhang et al., 2018) to identify CAZymes predicted to be extracellular. Out of the 193 identified predicted extracellular proteins, 105 were annotated as CAZymes, indicating a notable enrichment (for the predicted secretome, 22% of proteins are CAZymes). Among these, the majority (n=68; 65%), were identified as glycoside hydrolases (GHs). Notably, there was no CAZyme found in every single secretome. Thirty detected CAZymes were found only in the hemicellulose-containing substrates (Bark, ACB, GM), and these included 21 GHs. Growth on spruce bark involves the production of proteins specialized in the degradation of pectin, cellulose, starch, GAX, and GGM as is evident by the detection of multiple members of the glycoside hydrolase families GH28 (n=5), GH7 (n=3), GH31 (n=3), GH5_7 (n=2), and GH10 (n=4). This supports our data from the compositional analysis showing considerable degradation of these polysaccharides.

As expected, the secretomes for Bark, ACB, and cellulose contained multiple putative cellulose-degrading enzymes (Table 1), including β-glucosidases (GH3; n=3), cellobiohydrolases (GH6/GH7; n=4), endoglucanases (GH5/GH12; n=10), AA3 cellobiose dehydrogenases (CDH, AA3_1; n=1), and lytic polysaccharide monooxygenase (LPMOs; AA9, n=8). Remarkably, the secretomes for both bark substrates showed a higher number of AA9 LPMOs and cellobiohydrolases compared to the cellulose sample (Table 1; supplementary material). This difference may be attributed to the higher complexity of the bark substrate, leading to the production of more intricate enzymatic machineries. In this respect, it is noteworthy that AA9 LPMOs may act on various hemicelluloses and cellulose-hemicellulose assemblies (Hegnar et al., 2021; Hüttner et al., 2019; Tõlgo et al., 2022). Also, putative starch degrading enzymes were

detected, including α-amylase (GH13, n=2) and α-glucosidase (GH31, n=3) in the Bark, ACB, and GM proteomes.

Degradation of the main spruce bark hemicelluloses GGM and GAX involves various enzymes, and in the secretomes β-xylosidase/α-L-arabinofuranosidase (GH43; n=2), xylanase (GH10; n=4), endomannanase (GH5_7; n=2), β-mannosidase/glucosidase (GH2; n=1), acetylxylan esterase (CE2/CE4; n=2), and glucuronoyl esterases (CE15; n=7) were detected. Such enzymes were not found in the cellulose sample, but they did appear in the bark (non-extracted and ACB) and GM samples (Table 1), likely due to the presence of GGM and GAX in the bark. The CEs detected play a role in deacetylating polysaccharides and breaking lignin-carbohydrate linkages between hemicellulose and lignin, possibly contributing to better accessibility for backbone degrading enzymes (Larsbrink & Lo Leggio, 2023). Surprisingly, enzymes putatively acting on xyloglucan (XyG), were identified in all proteomes. This included xyloglucanases (GH74/GH44; n=2) and a fucosidase (GH95; n=1) putatively cleaving the β-(1→4)-linked glucan backbone and L-fucose decorations, respectively. XyG was relatively recently identified in spruce bark and is not typically associated with bark tissue (Kemppainen et al., 2014). The identification of enzymes capable of breaking down XyG during growth on bark serves as further evidence for the existence of XyG in spruce bark.

Enzymes involved in the removal of main chain decorations in pectin can be challenging to differentiate from hemicellulose-degrading enzymes due to shared structural elements. Predicted pectin-active CAZymes were identified, including polygalacturonases (GH28; n=5), pectin methylesterase (CE8; n=1), rhamnosidase (GH78; n=1), endoarabinanase (GH43; n=2), and rhamnogalacturonyl hydrolase (GH105; n=1). Interestingly, a larger number of proteins from these pectin-related families were identified in the two bark samples (Table 1), which corresponds well with pectin being a part of the bark matrix.

While Basidiomycetes are recognized for their ability to metabolize lignin, our analyses suggested lignin degradation to be limited during growth of *D. squalens* on bark and as discussed above, only 10% of ASL appeared to be removed over the six month-long experiment. Nevertheless, in the proteome analysis, predicted lignin-degrading enzymes were identified in both bark proteomes, with oxidoreductases (AA3_2; n=4), copper radical oxidases (AA5_1; n=2), and laccases (AA1; n=2). Surprisingly, five of these seven proteins were found in the GM as well as the two bark samples, possibly suggesting co-regulation of both GM- and lignin degradation processes. Putative chitinolytic enzymes were also detected, with β-*N*-acetylhexosaminidase (GH20; n=2), chitinase (GH18; n=3), α-*N*-acetylglucosaminidase (GH89; n=1), and chitin deacetylase esterase (CE4; n=1), identified in the Bark, ACB, and GM proteomes but not in the Cel or Glc proteomes. This is possibly a reflection of cell wall modification during fungal growth. A more comprehensive description of secreted proteins that were only detected in the two bark samples is provided below.

### *3.7 Extracellular proteins detected during growth on spruce bark*

Looking at all 193 proteins predicted to be secreted, 42 were exclusively identified in both bark samples (Fig. 4; see supplementary material) and 31 of these were annotated as CAZymes by dbCAN2 (Fig. 4). Fig. 4 provides an overview of these bark-exclusive secreted proteins, which may play a crucial role in the degradation of bark components such as extractives, GAX and pectin. Fewer proteins were detected in the ACB proteome compared to non-extracted bark, which could reflect that ACB is less complex. Many GHs (11 out of the 20 total detected GHs) were detected in both the extractive-free and the non-treated bark sample, and 8 exclusively in the latter. Only one GH, a putative GH115 α-glucuronidase (UniProt accession number; A0A4Q9PZ29) was exclusively found in the extracted bark.

As expected based on the observed degradation of GAX and pectin, some putative xylan and pectin degrading enzymes were identified only in the bark proteomes. Interestingly, several of these were not detected in the ACB proteome, including: α-(1→2)-L-fucosidase (GH95,

A0A4V2K8L7), α-L-rhamnosidase (GH78, A0A4Q9PG03), and polygalacturonase (GH28, A0A4Q9NRD1). As for xylan, two GH10 xylanases (A0A4Q9PNM1, A0A4V2K1M9) were found in both bark samples. Several GHs putatively related to fungal cell-wall modification were also identified, including an exo-α-(1→6)-mannosidase (GH125, A0A4Q9P6J3) and a chitinase (GH18, A0A4Q9PUY3). It is conceivable that the bark extractives induced lysis which stimulated the fungus to reinforce and/or adapt its cell wall, however the presence of these enzymes could also reflect general cell wall modification during growth.

Of the nine secreted proteins classified as auxiliary activity (AA) detected in the bark samples, six were found only in the non-extracted bark proteome. This includes 3 out of the 4 AA9 LPMOs (A0A4Q9PQC0, A0A4Q9Q8Z1, A0A4Q9QAL2). In contrast to GHs, LPMOs can specifically target and act on crystalline sections of polysaccharides (Vaaje-Kolstad et al., 2010). While LPMOs are commonly linked to cellulose degradation, recent research has unveiled their activity on cellulose-associated xylan (Frommhagen et al., 2015; Hegnar et al., 2021; Hüttner et al., 2019). Some AA9 LPMOs can also oxidize phenolic compounds or contribute indirectly by supplying other enzymes with $H_2O_2$ through their oxidase activity (Kracher et al., 2016; Li et al., 2021). The proteome from non-extracted bark contained additional $H_2O_2$-producing enzymes: AA3_2 glucose oxidase (A0A4Q9P514), AA5_1 glyoxal oxidase (A0A4Q9NTH3), and AA7 oligosaccharide oxidase (A0A4Q9MRJ0). Produced $H_2O_2$ could drive LMPO reactions (Bissaro et al., 2017), or enable unspecific Fenton reactions, previously demonstrated to lead to degradation of pine-derived extractives (Belt et al., 2017; Belt et al., 2022). Both LPMO and Fenton reactions also require reducing power that likely can be delivered by some of the extractives, as has been demonstrated for gallic acid (Golten et al., 2023). One laccase (AA1, A0A4Q9P7M4) was present in both bark samples, and could possibly be involved in conversion of lignin or, maybe more likely, extractives, as previously suggested (Gutiérrez et al., 2006; Valette et al., 2017).

Several proteins of unknown function were identified only in the bark samples (Fig. 4), which is a strong indication that they have bark-related functions. Eleven of the 42 bark-specific proteins do not have a CAZy annotation, and furthermore, seven of these were only found in the non-extracted bark sample. Some of these unstudied proteins were putatively annotated, and they may represent hitherto unknown carbohydrate-degrading or extractive-degrading functionalities (Fig. 4). Their putative annotations (based on Uniprot and dbCAN) include possible novel CAZymes, with a six-hairpin glycosidase-like protein (A0A4Q9PLQ5), a putative GH43 protein (A0A4Q9PS69), and a reducing-end specific xyloglucooligosaccharide hydrolase (A0A4Q9PAG2). Additionally, an uncharacterized protein (A0A4Q9PML4), two proteins with domains of unknown function (DUF) (A0A4Q9Q8S7, A0A4Q9P6Q6), and a cytochrome P450 (A0A4V2K8F9) were identified. The six-hairpin glycosidase-like protein A0A4Q9PLQ5 showed high sequence identity (75.84%) to a GH65 protein (A0A5C3PMI1) from *Polyporus arcularius*, which is the closest hit to a CAZyme in UniProt. However, it is important to note that the homologous *P. arcularius* GH65 protein has not been biochemically characterized, making the functional prediction of A0A4Q9PLQ5 speculative (of note, the GH65 family contains enzymes a wide variety of catalytic activities). The uncharacterized protein A0A4Q9PML4 has no clear functional prediction, but the closest hits to an AlphaFold structure prediction in Dali are a nuclease and a member from the Plant Invertase/Pectin Methylesterase Inhibitor superfamily (Holm, 2020). The top hits for the AlphaFold generated structure of A0A4Q9Q8S7 in Dali were a β-xylosidase and a glucosylceramidase (Holm, 2020). Based on InterPro analysis, the two DUF proteins A0A4Q9Q8S7 and A0A4Q9P6Q6 are categorized as components of the carbohydrate metabolic process. These proteins are actually comprised of three DUFs (DUF5127, DUF4965, DUF1793; Pfam: PF17168, PF16335, PF08760), with the two C-terminal domains partially associated with the superfamily of six-hairpin glycosidases (residues 391-582). The two DUF-domain proteins have a similar architecture as WP_074995790 from the bacterium *Streptomyces misionensis*, and this protein has been demonstrated to have weak β-galactosidase activity

(Schmerling et al., 2022). Possibly, A0A4Q9Q8S7 and A0A4Q9P6Q6 from *D. squalens* also function as GHs.

Although assignment of functionality requires biochemical characterization, the above considerations suggest that several of the proteins with unknown function detected in the bark secretomes are involved in carbohydrate turnover. The only, and notable, clear exception is the cytochrome P450 protein, A0A4V2K8F9, which was only found with non-extracted bark. Cytochrome P450s catalyze a wide range of oxidations, and as many are known to have detoxifying roles (Torres et al., 2003), and as such a putative role of A0A4V2K8F9 might be in the modification of spruce extractives. Previously, *R. placenta* was shown to upregulate several cytochrome P450s during growth on pinewood, suggesting that oxidative processes are important during growth on softwood biomass (Vanden Wymelenberg et al., 2011) .

## 4. Conclusions

Understanding microbial degradation of bark is fundamental in developing biological utilization processes. We show that fungi from various taxonomic groups can grow on spruce bark, and that they exhibit different growth and degradation strategies. Among the fungi examined, *D. squalens, T. reesei,* and *Trichoderma* sp. B1 were the most efficient in overall bark degradation, especially regarding extractives, pectin, GAX, and starch. Furthermore, proteomics analysis of *D. squalens* implicated multiple putative CAZymes and proteins of unknown function that could be involved in polysaccharide and extractive degradation. This work provides a foundation for further valorization of this abundant renewable resource.

E-supplementary data of this work can be found in online version of the paper.

## AUTHOR STATEMENTS

### *Declaration of competing interest*

The authors declare no conflicts of interest.

### *Data availability*

*Trichoderma* sp. B1, and its ITS and EF1-α sequences have been deposited in NCBI under accession numbers OQ875786 and OQ918064. The proteomics data have been deposited to the ProteomeXchange Consortium via the PRIDE (Perez-Riverol et al., 2022) partner repository with the dataset identifier PXD043339.

## References


Arntzen, M.Ø., Bengtsson, O., Várnai, A., Delogu, F., Mathiesen, G., Eijsink, V.G.H. 2020. Quantitative comparison of the biomass-degrading enzyme repertoires of five filamentous fungi. *Scientific Reports*, **10**(1), 20267.

Belt, T., Hänninen, T., Rautkari, L. 2017. Antioxidant activity of Scots pine heartwood and knot extractives and implications for resistance to brown rot. *Holzforschung*, **71**(6), 527-534.

Belt, T., Harju, A., Kilpeläinen, P., Venäläinen, M. 2022. Fungal degradation of extractives plays an important role in the brown rot decay of Scots pine heartwood. *Frontiers in Plant Science*, 1574.

Bengtsson, O., Arntzen, M.Ø., Mathiesen, G., Skaugen, M., Eijsink, V.G.H. 2016. A novel proteomics sample preparation method for secretome analysis of *Hypocrea jecorina* growing on insoluble substrates. *Journal of Proteomics*, **131**, 104-112.

Bissaro, B., Røhr, Å.K., Müller, G., Chylenski, P., Skaugen, M., Forsberg, Z., Horn, S.J., Vaaje-Kolstad, G., Eijsink, V.G. 2017. Oxidative cleavage of polysaccharides by monocopper enzymes depends on $H_2O_2$. *Nature chemical biology*, **13**(10), 1123-1128.

Carbone, I., Kohn, L.M. 1999. A method for designing primer sets for speciation studies in filamentous ascomycetes. *Mycologia*, **91**(3), 553-556.

Clarke, J., Davidson, K., Rixon, J., Halstead, J., Fransen, M., Gilbert, H., Hazlewood, G. 2000. A comparison of enzyme-aided bleaching of softwood paper pulp using combinations of xylanase, mannanase and α-galactosidase. *Applied Microbiology and Biotechnology*, **53**, 661-667.

Daly, P., López, S.C., Peng, M., Lancefield, C.S., Purvine, S.O., Kim, Y.M., Zink, E.M., Dohnalkova, A., Singan, V.R., Lipzen, A. 2018. *Dichomitus squalens* partially tailors its molecular responses to the composition of solid wood. *Environmental microbiology*, **20**(11), 4141-4156.

Ek, M., Gellerstedt, G., Henriksson, G. 2009. *Wood chemistry and biotechnology*. Walter de Gruyter.

Fengel, D., Wegener, G. 1984. in: *Wood: chemistry, ultrastructure, reactions*, (Eds.) D. Fengel, G. Wegener, Walter de Gruyter, pp. 227-238.

Frommhagen, M., Sforza, S., Westphal, A.H., Visser, J., Hinz, S.W., Koetsier, M.J., van Berkel, W.J., Gruppen, H., Kabel, M.A. 2015. Discovery of the combined oxidative cleavage of plant xylan and cellulose by a new fungal polysaccharide monooxygenase. *Biotechnology for Biofuels*, **8**(1), 1-12.

Gao, L., Liu, G., Zhao, Q., Xiao, Z., Sun, W., Hao, X., Liu, X., Zhang, Z., Zhang, P. 2022. Customized optimization of lignocellulolytic enzyme cocktails for efficient conversion of pectin-rich biomass residues. *Carbohydr Polym*, **297**, 120025.

Golten, O., Ayuso-Fernández, I., Hall, K.R., Stepnov, A.A., Sørlie, M., Røhr, Å.K., Eijsink, V.G. 2023. Reductants fuel lytic polysaccharide monooxygenase activity in a pH-dependent manner. *FEBS letters*, 1363-1374.

Gutiérrez, A., del Río, J.C., Rencoret, J., Ibarra, D., Martínez, Á.T. 2006. Main lipophilic extractives in different paper pulp types can be removed using the laccase–mediator system. *Applied Microbiology and Biotechnology*, **72**(4), 845-851.

Hegnar, O.A., Østby, H., Petrović, D.M., Olsson, L., Várnai, A., Eijsink, V.G. 2021. Quantifying oxidation of cellulose-associated glucuronoxylan by two lytic polysaccharide monooxygenases from *Neurospora crassa*. *Applied and Environmental Microbiology*, **87**(24), e01652-21.

Holm, L. 2020. DALI and the persistence of protein shape. *Protein Science*, **29**(1), 128-140.

Hori, C., Ishida, T., Igarashi, K., Samejima, M., Suzuki, H., Master, E., Ferreira, P., Ruiz-Dueñas, F.J., Held, B., Canessa, P. 2014. Analysis of the *Phlebiopsis gigantea* genome, transcriptome and secretome provides insight into its pioneer colonization strategies of wood. *PLoS Genetics*, **10**(12), e1004759.

Horton, P., Park, K.-J., Obayashi, T., Fujita, N., Harada, H., Adams-Collier, C., Nakai, K. 2007. WoLF PSORT: protein localization predictor. *Nucleic acids research*, **35**, W585-W587.

Hüttner, S., Várnai, A., Petrović, D.M., Bach, C.X., Kim Anh, D.T., Thanh, V.N., Eijsink, V.G., Larsbrink, J., Olsson, L. 2019. Specific xylan activity revealed for AA9 lytic polysaccharide monooxygenases of the thermophilic fungus *Malbranchea cinnamomea* by functional characterization. *Applied and Environmental Microbiology*, **85**(23), e01408-19.

Jaklitsch, W.M., Komon, M., Kubicek, C.P., Druzhinina, I.S. 2005. *Hypocrea voglmayrii* sp. nov. from the Austrian Alps represents a new phylogenetic clade in *Hypocrea/Trichoderma*. *Mycologia*, **97**(6), 1365-1378.

Jones, D.B. 1931. *Factors for converting percentages of nitrogen in foods and feeds into percentages of proteins*. US Department of Agriculture.

Käll, L., Krogh, A., Sonnhammer, E.L. 2004. A combined transmembrane topology and signal peptide prediction method. *Journal of molecular biology*, **338**(5), 1027-1036.

Kemppainen, K., Siika-aho, M., Pattathil, S., Giovando, S., Kruus, K. 2014. Spruce bark as an industrial source of condensed tannins and non-cellulosic sugars. *Industrial Crops and Products*, **52**, 158-168.

Kirker, G.T., Blodgett, A.B., Arango, R.A., Lebow, P.K., Clausen, C.A. 2013. The role of extractives in naturally durable wood species. *International Biodeterioration & Biodegradation*, **82**, 53-58.

Kracher, D., Scheiblbrandner, S., Felice, A.K., Breslmayr, E., Preims, M., Ludwicka, K., Haltrich, D., Eijsink, V.G., Ludwig, R. 2016. Extracellular electron transfer systems fuel cellulose oxidative degradation. *Science*, **352**(6289), 1098-1101.

Krogell, J., Holmbom, B., Pranovich, A., Hemming, J., Willför, S. 2012. Extraction and chemical characterization of Norway spruce inner and outer bark. *Nordic Pulp & Paper Research Journal*, **27**(1), 6-17.

Krogell, J., Korotkova, E., Eränen, K., Pranovich, A., Salmi, T., Murzin, D., Willför, S. 2013. Intensification of hemicellulose hot-water extraction from spruce wood in a batch extractor – Effects of wood particle size. *Bioresource Technology*, **143**, 212-220.

Kubicek, C.P. 2012. The actors: plant biomass degradation by fungi. 1st ed. in: *Fungi and Lignocellulosic Biomass*, John Wiley & Sons, Incorporated, pp. 29-44.

Kwan, I., Huang, T., Ek, M., Seppänen, R., Skagerlind, P. 2022. Bark from Nordic tree species – a sustainable source for amphiphilic polymers and surfactants. *Nordic Pulp & Paper Research Journal*, **37**(4), 566-575.

Larsbrink, J., Lo Leggio, L. 2023. Glucuronoyl esterases - enzymes to decouple lignin and carbohydrates and enable better utilization of renewable plant biomass. *Essays Biochem*, **67**(3), 493-503.

Le Normand, M., Edlund, U., Holmbom, B., Ek, M. 2012. Hot-water extraction and characterization of spruce bark non-cellulosic polysaccharides. *Nordic Pulp & Paper Research Journal*, **27**(1), 18-23.

Le Normand, M., Rietzler, B., Vilaplana, F., Ek, M. 2021. Macromolecular model of the pectic polysaccharides isolated from the bark of Norway spruce (*Picea abies*). *Polymers*, **13**(7), 1106.

Li, F., Zhao, H., Shao, R., Zhang, X., Yu, H. 2021. Enhanced Fenton reaction for xenobiotic compounds and lignin degradation fueled by quinone redox cycling by lytic polysaccharide monooxygenases. *Journal of Agricultural and Food Chemistry*, **69**(25), 7104-7114.

Lorentzen, S.B., Arntzen, M.Ø., Hahn, T., Tuveng, T.R., Sørlie, M., Zibek, S., Vaaje-Kolstad, G., Eijsink, V.G.H. 2021. Genomic and proteomic study of *Andreprevotia ripae* isolated from an anthill reveals an extensive repertoire of chitinolytic enzymes. *Journal of Proteome Research*, **20**(8), 4041-4052.

Martin, K.J., Rygiewicz, P.T. 2005. Fungal-specific PCR primers developed for analysis of the ITS region of environmental DNA extracts. *BMC microbiology*, **5**(1), 1-11.

Martin, V.J., Yu, Z., Mohn, W.W. 1999. Recent advances in understanding resin acid biodegradation: microbial diversity and metabolism. *Archives of Microbiology*, **172**(3), 131-138.

Martins, I., Garcia, H., Varela, A., Núñez, O., Planchon, S., Galceran, M.T., Renaut, J., Rebelo, L.P.N., Silva Pereira, C. 2014. Investigating *Aspergillus nidulans* secretome during colonisation of cork cell walls. *Journal of Proteomics*, **98**, 175-188.

Perez-Riverol, Y., Bai, J., Bandla, C., García-Seisdedos, D., Hewapathirana, S., Kamatchinathan, S., Kundu, D.J., Prakash, A., Frericks-Zipper, A., Eisenacher, M. 2022. The PRIDE database resources in 2022: a hub for mass spectrometry-based proteomics evidences. *Nucleic acids research*, **50**(D1), D543-D552.

Ristinmaa, A.S., Tafur Rangel, A., Idström, A., Valenzuela, S., Kerkhoven, E.J., Pope, P., Hasani, M., Larsbrink, J. 2023. Resin acids play key roles in shaping microbial communities during degradation of spruce bark. *bioRxiv*, 2023.04. 19.537524.

Schmerling, C., Sewald, L., Heilmann, G., Witfeld, F., Begerow, D., Jensen, K., Bräsen, C., Kaschani, F., Overkleeft, H.S., Siebers, B., Kaiser, M. 2022. Identification of fungal lignocellulose-degrading biocatalysts secreted by *Phanerochaete chrysosporium* via activity-based protein profiling. *Communications Biology*, **5**(1), 1254.

Teufel, F., Almagro Armenteros, J.J., Johansen, A.R., Gíslason, M.H., Pihl, S.I., Tsirigos, K.D., Winther, O., Brunak, S., von Heijne, G., Nielsen, H. 2022. SignalP 6.0 predicts all five types of signal peptides using protein language models. *Nature biotechnology*, **40**(7), 1023-1025.

Tõlgo, M., Hegnar, O.A., Østby, H., Várnai, A., Vilaplana, F., Eijsink, V.G., Olsson, L. 2022. Comparison of six lytic polysaccharide monooxygenases from *Thermothielavioides terrestris* shows that functional variation underlies the multiplicity of LPMO genes in filamentous fungi. *Applied and Environmental Microbiology*, **88**(6), e00096-22.

Torres, E., Bustos-Jaimes, I., Le Borgne, S. 2003. Potential use of oxidative enzymes for the detoxification of organic pollutants. *Applied Catalysis B: Environmental*, **46**(1), 1-15.

Vaaje-Kolstad, G., Westereng, B., Horn, S.J., Liu, Z., Zhai, H., Sørlie, M., Eijsink, V.G. 2010. An oxidative enzyme boosting the enzymatic conversion of recalcitrant polysaccharides. *Science*, **330**(6001), 219-222.

Valentín, L., Kluczek-Turpeinen, B., Willför, S., Hemming, J., Hatakka, A., Steffen, K., Tuomela, M. 2010. Scots pine (*Pinus sylvestris*) bark composition and degradation by fungi: Potential substrate for bioremediation. *Bioresource Technology*, **101**(7), 2203-2209.

Valette, N., Perrot, T., Sormani, R., Gelhaye, E., Morel-Rouhier, M. 2017. Antifungal activities of wood extractives. *Fungal Biology Reviews*, **31**(3), 113-123.

van Erven, G., de Visser, R., Merkx, D.W.H., Strolenberg, W., de Gijsel, P., Gruppen, H., Kabel, M.A. 2017. Quantification of lignin and its structural features in plant biomass using 13C lignin as internal standard for pyrolysis-GC-SIM-MS. *Analytical Chemistry*, **89**(20), 10907-10916.

Vanden Wymelenberg, A., Gaskell, J., Mozuch, M., BonDurant, S.S., Sabat, G., Ralph, J., Skyba, O., Mansfield, S.D., Blanchette, R.A., Grigoriev, I.V., Kersten, P.J., Cullen, D. 2011. Significant alteration of gene expression in wood decay fungi *Postia placenta* and *Phanerochaete chrysosporium* by plant species. *Appl Environ Microbiol*, **77**(13), 4499-507.

Yadav, K., Yadav, S., Anand, G., Yadav, P.K., Yadav, D. 2023. Hydrolysis of complex pectin structures: Biocatalysis and bioproducts. in: *Polysaccharide Degrading Biocatalysts*, Elsevier, pp. 205-225.

Zhang, H., Yohe, T., Huang, L., Entwistle, S., Wu, P., Yang, Z., Busk, P.K., Xu, Y., Yin, Y. 2018. dbCAN2: a meta server for automated carbohydrate-active enzyme annotation. *Nucleic acids research*, **46**(W1), W95-W101.

## Figure Captions

**Figure 1. Growth of filamentous fungi on spruce bark over six months (24 weeks), with the bark as the sole carbon source**. No fungus was added to the blank sample. The plates were incubated at 20 °C. A) Representative plates from growth on bark. B) Mass loss for the different fungi. Individual data point measurements from biological duplicate experiments are shown and the line displays the mean.

**Figure 2.** Effect of fungal treatment on bark components over 24 weeks of growth. A) Percent change in ash content in each chemically analyzed sample, showing a consistent increase across all samples subjected to fungal treatment. Panels B – E show the percent change in acid soluble lignin (B; ASL), acetone extractives (C), protein (D) Klason lignin (E) content after 12 and 24 weeks. Panel F shows the effect of fungal growth on the content of selected extractive compounds after 12 and 24 weeks of growth. This panel shows that fungal treatment led to decreases in the three fatty acids, hexadecanoic acid, 9,12-octadecadienoic acid and trans-9-octadecenoic acid, across all samples. The resin acids dehydroabietic acid, acid, abietic acid, pimaric acid all decreased in the bark samples treated with the two Basidiomycetes *D. squalens* and *R. placenta*,

773 while little to no change was observed for the three fungi from the Ascomycota phylum. 7-
774 oxodehydroabieitic acid was not identified in the bark samples treated with *D. squalens* or *R.*
775 *placenta*. β-sitosterol increased in samples treated with *D. squalens*, *P. crustosum* and
776 *Trichoderma* sp. B1 and was only degraded by *T. reesei*.

777

778 **Figure 3**. Effect of fungal treatment on the arabinose, galactose, glucose (corr) = glucose
779 corrected for measured glucose from starch, glucose (starch) = measured starch content, mannose,
780 rhamnose, and xylose composition of the bark after 12 and 24 weeks of fungal growth. The values
781 were normalized against the total amount of ash, with the percent change relative to the blank
782 sample for each timepoint (Equation 1). Data points from biological triplicate experiments are
783 shown, as well as means and error bars showing standard errors. Data for the control (blank)
784 sample are shown in the supplementary material.

785

786 **Figure 4.** Proteins predicted to be secreted and that were identified in the secretome of *D.*
787 *squalens* during growth on bark or acetone-extracted bark (ACB). A) List of the secreted proteins
788 only detected in one or both of the bark proteomes. Proteins that were not detected on a specific
789 carbon source are colored grey in the grid and proteins detected are colored blue. Protein
790 accession numbers (Uniprot), CAZy annotations (by dbCAN2) and protein names (from Uniprot)
791 (note that there are some minor inconsistencies between the Uniprot- and dbCAN2-based
792 annotations). When applicable, the CAZy class is indicated in the right column by color: AA
793 (auxiliary activity) in pink, CE (carbohydrate esterase) in green, GH (glycoside hydrolase) in
794 blue, N/A in grey. The higher abundance and diversity of secreted proteins during growth on
795 intact bark compared to extractive-free bark is apparent, both regarding putative hydrolases and
796 oxidoreductases. B) Domain architecture of five hypothetical proteins only found in one or both

797 of the bark proteomes (indicated in bold in A). Signal peptides are shown in yellow. DUF =
798 domain of unknown function.

799

800

## Tables and Figures

**Table 1.** CAZymes identified in the *D. squalens* secretomes from growth on acetone-extracted bark (ACB), non-extracted bark (Bark), galactomannan (GM), cellulose (Cel) or glucose (Glc). The Table shows all CAZy families of which at least one member was detected and the number of identified members per family (see supplementary information). Abbreviations: AA, auxiliary activity; CE, carbohydrate esterase; GH, glycoside hydrolase. No Polysaccharide Lyases were detected.

| Polysaccharide | CAZy family | ACB | Bark | GM | Cel | Glc |
|---|---|---|---|---|---|---|
| Cellulose | GH3*, 5, 6, 7 12, 44 | 14 | 15 | 11 | 6 | 0 |
| | AA9, AA3_1 | 5 | 9 | 3 | 2 | 0 |
| Starch | GH13, 31* | 1 | 2 | 3 | 0 | 0 |
| Xylan | GH10 | 3 | 4 | 0 | 0 | 0 |
| | CE2, 4, 15, 16 | 5 | 11 | 12 | 0 | 1 |
| Xyloglucan | GH35, 74, 95, 12 | 5 | 4 | 4 | 2 | 1 |
| Mannan | GH5_7, 27 | 3 | 5 | 5 | 1 | 0 |
| Pectin | CE8 | 0 | 1 | 1 | 0 | 0 |
| | GH28, 105, 43*, 53, 78 | 7 | 10 | 6 | 0 | 0 |
| Lignin | AA1, 3_2, 5_1 | 5 | 6 | 5 | 0 | 0 |

* These CAZyme families contain members with other activities, meaning that the detected proteins could potentially be involved in depolymerization of other polysaccharides.

811 ***Figure 1***

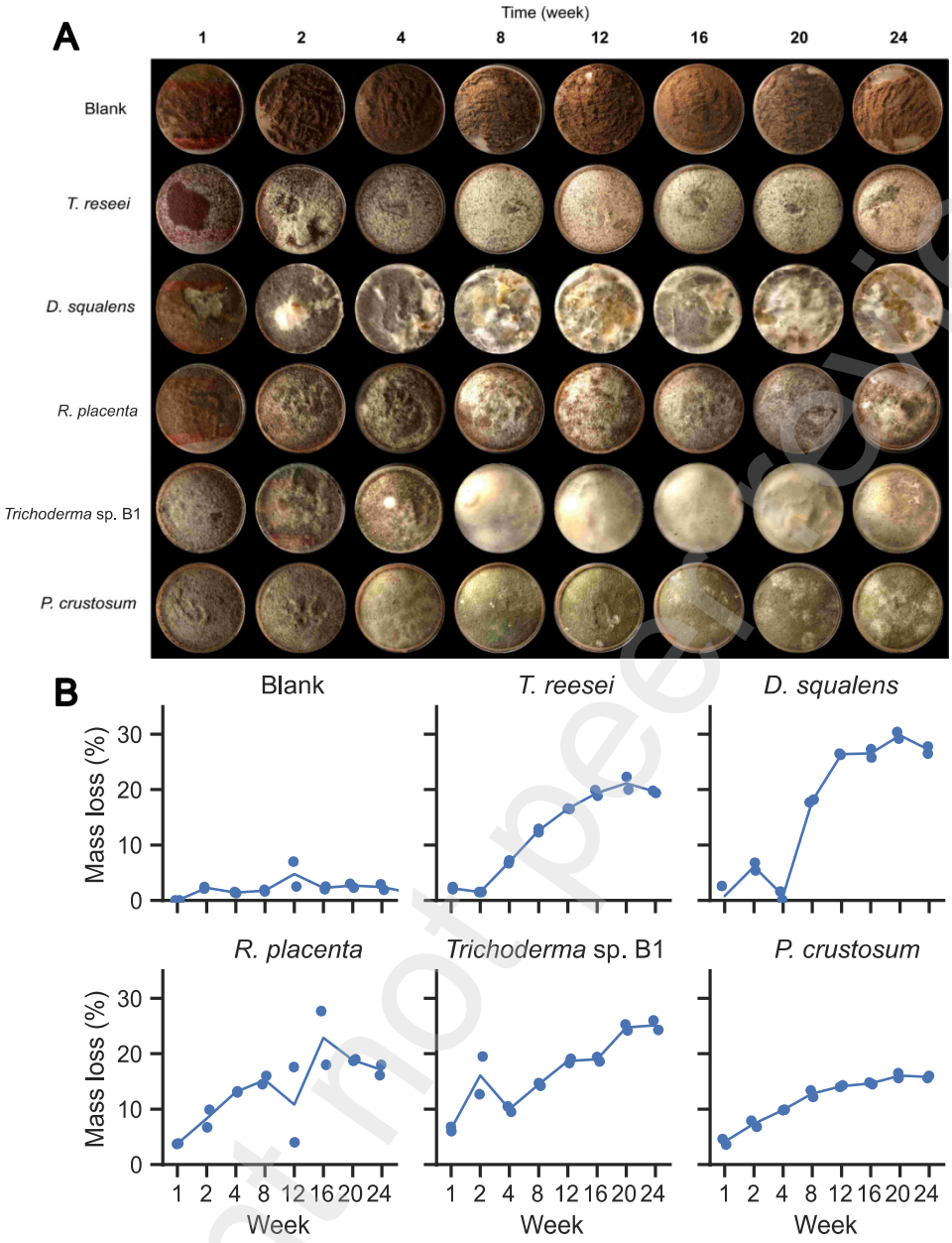


812

813

814 ***Figure 2***

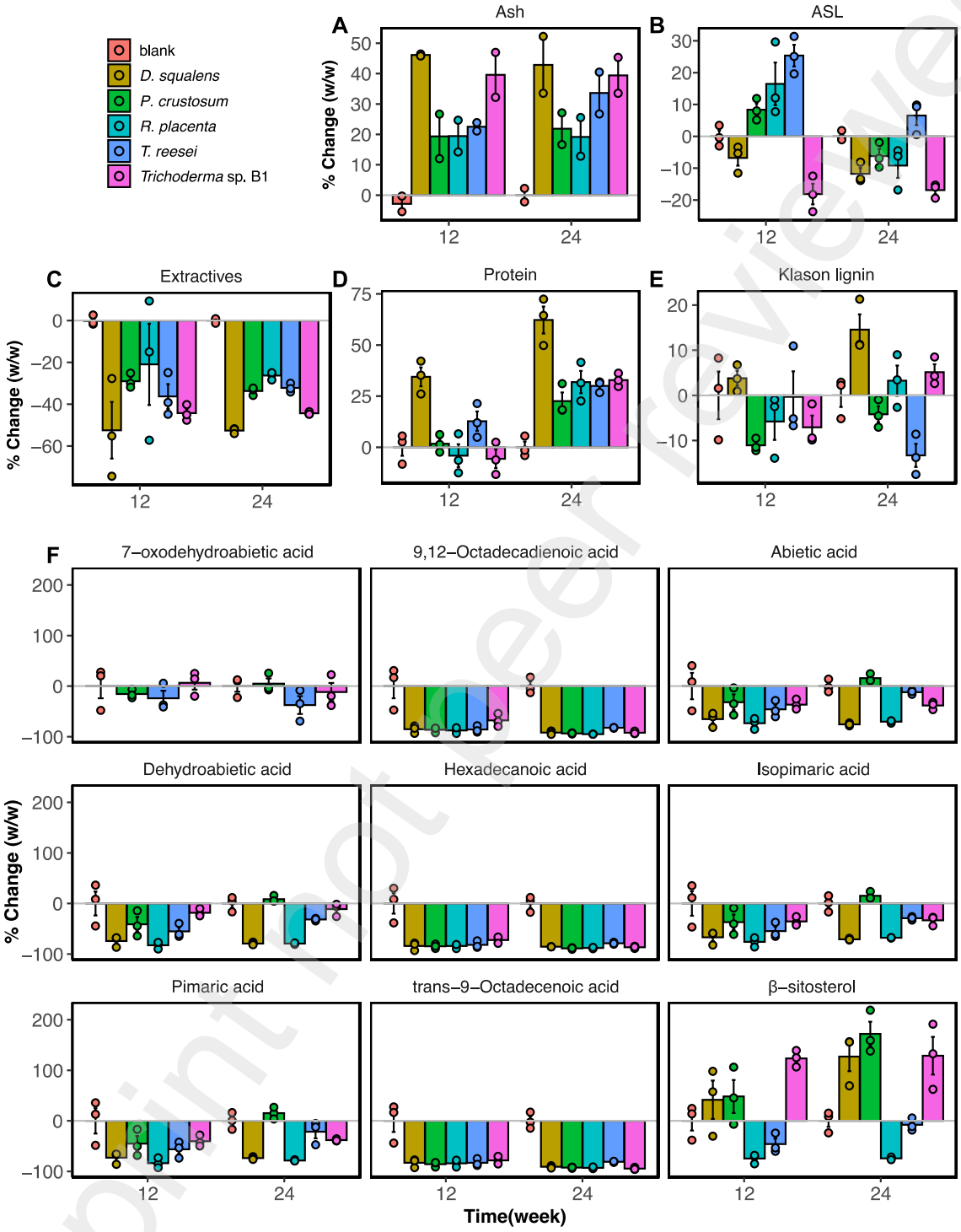


815

816

817 ***Figure 3***

818

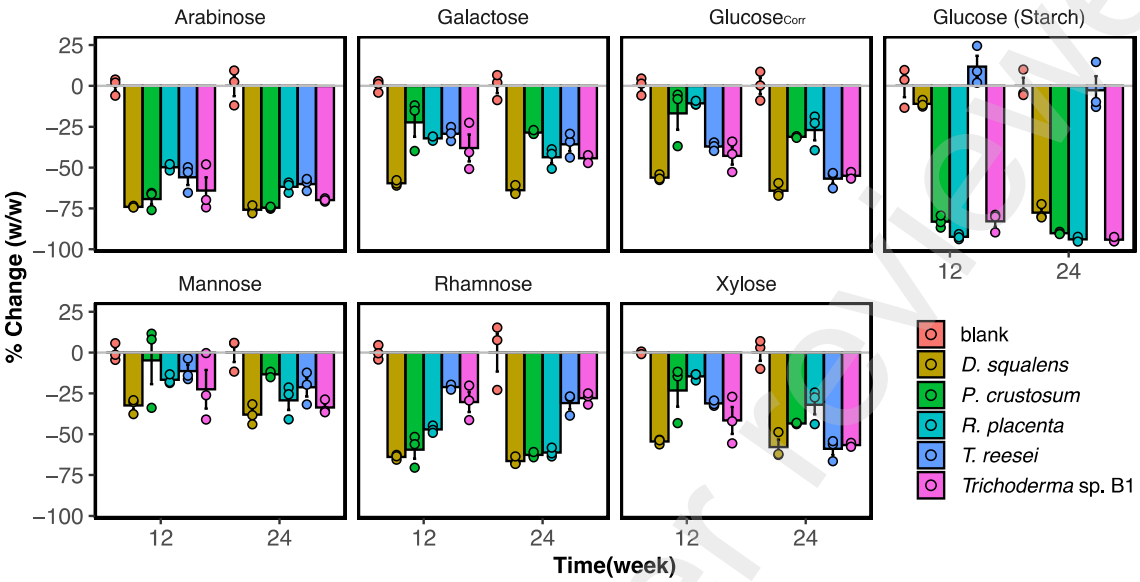


819
820

821 ***Figure 4***

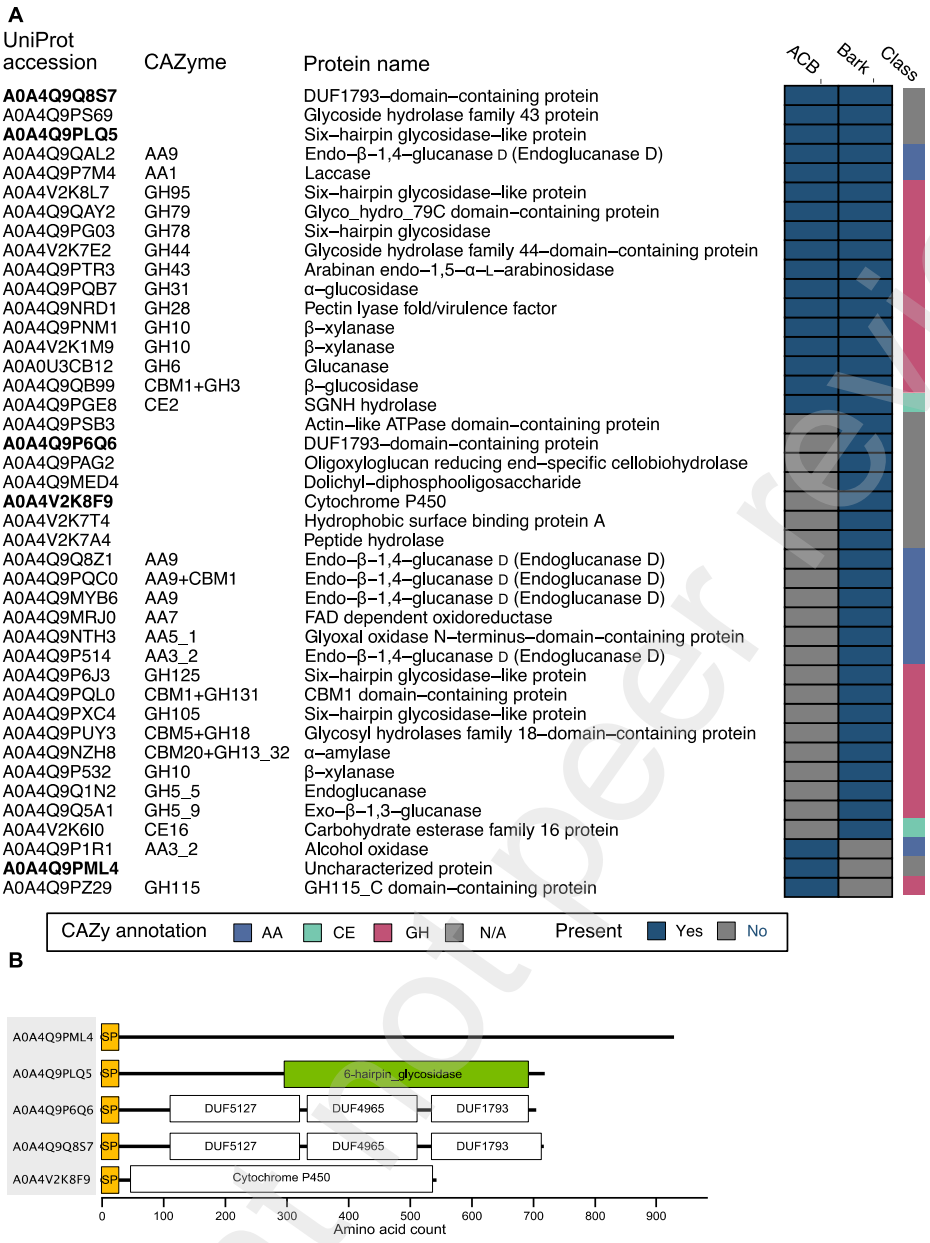


822